Original Article

Alterations of interhemispheric functional homotopic connectivity and corpus callosum microstructure in bulimia nervosa

Yiling Wang[1#], Lirong Tang[2#], Miao Wang[3], Weihua Li[1], Xuemei Wang[2], Jiani Wang[1], Qian Chen[1], Zhenghan Yang[1], Xiaohong Li[2], Zhanjiang Li[2], Guowei Wu[4], Peng Zhang[1], Zhenchang Wang[1]

[1]Department of Radiology, Beijing Friendship Hospital, Capital Medical University, Beijing, China; [2]The National Clinical Research Center for Mental Disorders & Beijing Key Laboratory of Mental Disorders, Beijing Anding Hospital, Capital Medical University, Beijing, China; [3]Chinese Institute for Brain Research, Beijing, China; [4]CAS Key Laboratory of Behavioral Science, Institute of Psychology, Chinese Academy of Sciences, Beijing, China

Contributions: (I) Conception and design: Y Wang, L Tang, P Zhang, G Wu, Z Wang; (II) Administrative support: Z Yang, X Li, Z Li, P Zhang, Z Wang; (III) Provision of study materials or patients: L Tang, X Wang, X Li, Z Li; (IV) Collection and assembly of data: Y Wang, W Li, J Wang, Q Chen, P Zhang; (V) Data analysis and interpretation: Y Wang, M Wang, G Wu, P Zhang; (VI) Manuscript writing: All authors; (VII) Final approval of manuscript: All authors.

[#]The authors contributed equally to this work.

Correspondence to: Peng Zhang, MD. Department of Radiology, Beijing Friendship Hospital, Capital Medical University, No. 95 Yongan Road, Xicheng District, Beijing 100050, China. Email: zpqz1021@foxmail.com; Guowei Wu, MS. CAS Key Laboratory of Behavioral Science, Institute of Psychology, Chinese Academy of Sciences, No. 16 Lincui Road, Chaoyang District, Beijing 100000, China. Email: wugw@psych.ac.cn; Zhenchang Wang, MD. Department of Radiology, Beijing Friendship Hospital, Capital Medical University, No. 95 Yongan Road, Xicheng District, Beijing 100050, China. Email: cjr.wzhch@vip.163.com.

Background: Accumulating evidence indicates maladaptive neural information interactions between different brain regions underlie bulimia nervosa (BN). However, little is known about the alterations in interhemispheric communication of BN, which is facilitated by the corpus callosum (CC), the major commissural fiber connecting the two hemispheres. To shed light on the interhemispheric communications in BN, the present study aims to explore alterations of interhemispheric homotopic functional connectivity and the CC microstructure in BN.

Methods: Based on magnetic resonance imaging (MRI) data collected from 42 BN patients and 38 healthy controls (HCs), the group differences of voxel-mirrored homotopic connectivity (VMHC) index and CC white matter microstructure were compared. Then brain regions with significant group differences in VMHC were selected as seeds for subsequent functional connectivity (FC) analysis. Seed-based fiber tracking and correlation analysis were used to analyze the relationship between VMHC and CC changes. And correlation analysis was used to reveal the correlation between abnormal imaging variables and the clinical features of BN.

Results: Compared with HCs, the BN group showed decreased fractional anisotropy (FA) in middle part of CC (CCMid) and increased VMHC in bilateral orbitofrontal cortex (OFC) and middle temporal gyrus (MTG) [false discovery rate (FDR) correction with a corrected threshold of $P<0.05$]. Subsequent FC analyses indicated increased FC between left OFC and right OFC, bilateral MTG, left middle occipital gyrus and right precuneus (PCUN); between right OFC and left cerebellum crus II and right PCUN; and between left MTG and right inferior temporal gyrus, right cerebellum lobule VI and right medial superior frontal gyrus (FDR correction with a corrected threshold of $P<0.05$). The VMHC values of OFC and MTG showed no correlations with FA values of the CCMid and the white fibers between the bilateral OFC and MTG were not through the CCMid. In addition, several regions with abnormal FC had a potential correlation trend with abnormal eating behaviors in BN patients ($P<0.05$, uncorrected).

Conclusions: Aberrant interhemispheric homotopic functional connectivity and CC microstructure were observed in BN, and they may be independent of each other. Regions with aberrant interhemispheric homotopic functional connectivity showed hyperconnectivity with regions related to reward processing, body shape perception, and self-reference.

Keywords: Bulimia nervosa (BN); interhemispheric communication; corpus callosum (CC); voxel-mirrored homotopic connectivity (VMHC); functional connectivity (FC)

Introduction

Bulimia nervosa (BN) is an refractory eating disorder characterized by recurrent binge-eating episodes, undue compensatory purging behavior, reduced self-regulatory capacity and preoccupation and dissatisfaction with body shape (1). Approximately 1% of young women are affected by BN, but the available treatments, both cognitive behavior therapy and pharmacotherapy, have a low remission rate of 30–40% at most (2,3). The vague neurobiological underpinnings have greatly hindered the development of precise treatments for this disease (4).

In recent years, advanced magnetic resonance imaging (MRI) techniques have been used to study BN, gradually elucidating the neural substrates underlying this complex and multidimensional psychopathological disorder. For example, some studies have consistently reported that frontostriatal activations in response to food cues were related to increased reward sensitivity and repeated bingeing behavior in BN (5,6). Uher *et al.* demonstrated diminished occipitotemporal responses in patients with BN when viewing their own abnormal body weight (7). Using the resting-state fMRI images (rs-fMRI), our previous study suggested aberrant regional activity in the left insula and bilateral inferior parietal lobule (8). Moreover, there is growing recognition that BN may result from abnormal information interaction between different functional centers or even across large-scale brain networks. Using seed-based functional connectivity (FC) analysis, a previous study reported correlations between the striatal subregions and frontal cortex (9). In addition, several brain sub-networks, such as the attention network, default mode network (DMN) (10), visual network and sensorimotor network (11), appeared disrupted in BN, indicating abnormal neural connections among diverse brain regions. However, neural communication between the two hemispheres in BN

remains largely unknown. Interhemispheric homotopic FC is a feature widely used to characterize interhemispheric communications, a fundamental property of brain networks (12) that indicates the functional coordination of the two hemispheres. This type of connectivity is primarily mediated by the corpus callosum (CC), a major commissure connecting the two hemispheres that facilitates interhemispheric information transmission (13,14). The CC is widely reported to be implicated in the pathogenesis of psychosis in neuroimaging studies (13,14). Furthermore, structural alterations in the CC have been supposed to the structural basis for altered interhemispheric interaction (15). Interhemispheric communication ensures that network information is reliably integrated (16,17) and plays a crucial role in diverse higher-level functions, such as interception, self-regulation and impulse control (14,18), consistent with the prominent behavioral deficits observed in BN. Elucidating the characteristics of interhemispheric communication may help to reveal the neural mechanism of BN and seek targets for its neuromodulation (such as transcranial magnetic stimulation and deep brain stimulation).

To address the gap in interhemispheric communication of BN, voxel-mirrored homotopic connectivity (VMHC) (16), corresponding seed-based FC analysis, diffusion tensor imaging (DTI) analysis, and a series of behavioral assessments were employed to explore the alterations of interhemispheric homotopic FC and abnormalities in white matter (WM) of CC, and their potential correlations with behaviors in BN. Our hypotheses were as follows: (I) patients with BN have aberrant interhemispheric communications in the perspective of interhemispheric homotopic FC and CC WM microstructure, and there is a potential correlation between them; (II) alterations of interhemispheric connectivity are associated with abnormal

behavioral features, and altered WM microstructure of CC may mediate the influence of interhemispheric functional connectivity on behaviors.

Methods

The study was conducted in accordance with the Declaration of Helsinki (as revised in 2013). The study was approved by the Ethics Committee of the Beijing Friendship Hospital (No. 2021-P2-052-01). All participants signed written informed consent.

Participants

Fifty BN patients were recruited from outpatient services and forty age-, sex- and education-matched healthy controls (HCs) were recruited by internet advertising. All participants were right-handed. Two psychiatrists with expertise in eating disorders independently made the diagnosis of BN using the Mini International Neuropsychiatric Interview (MINI) (19), a short-structured interview developed in accordance with the criteria of the Diagnostic and Statistical Manual of Mental Disorders, Fifth Edition (DSM-5). Patients were excluded if they were currently diagnosed with other major psychiatric disorders other than major depression and anxiety disorder (e.g., bipolar disorder, schizophrenia, etc.). Of the 50 BN patients, 3 had previously used anxiolytics, and 2 had previously taken antidepressants, but none had taken psychotropic drugs for at least two months prior to the study. 12 patients had a previous history of anorexia nervosa (AN).

HCs were required to have a normal weight and no previous history of psychiatric disorders. In addition, the MINI was also administered to each HC to exclude those with any potential psychiatric disorders.

Other exclusion criteria for both the BN and HC groups included: history of nicotine, alcohol, or other substance abuse disorders; history of traumatic brain injury, brain surgery, neurological disorders, pervasive developmental disorders and mental retardation; suffered from some major health problems (e.g., diabetes, hyperthyroidism, or hyperlipidemia, or chronic diseases, such as hypertension); were pregnant or lactating; were claustrophobia; and had any metal implants (contraindication for MRI). In this step, we excluded a total of 6 BN patients, two due to the history of alcoholic abuse, one due to the history of nicotine abuse, two due to metal implants and one due to claustrophobia. One HC was excluded because of the metal implant. Thus,

a total of 44 BN patients and 39 HCs remained for the next procedures.

Clinical data collection

All participants were required to fast for at least 4 hours before they arrived for the scanning visits. Participants were scheduled to complete several self-report questionnaires before their MRI scans. The Visual Analog Scale (VAS) was used to rate their current degrees of hunger on a scale from 0 ("not at all") to 10 ("extremely"). All participants then completed the Chinese version of the Dutch Eating Behavior Questionnaire (DEBQ) (20), the bulimia subscale of the Eating Disorders Questionnaire (EDI-BN) (21), the Eating Attitudes Test (EAT-26) (22), the Beck Depression Inventory (BDI) (23) and the Self-Assessment of Anxiety Scale (SAS) (24). The DEBQ is a scale that assesses eating behavior and consists of 33 items, including three subscales that reflect restrained, emotional and external eating. The EDI-BN, a subscale consisting of 7 items, was used to evaluate the drive for bulimia. The 26-item EAT-26 was applied to assess disturbed eating attitudes and behaviors. And the BDI and SAS were used to evaluate participants' depressive and anxiety states respectively. Previous studies have verified that these questionnaires have achieved good reliability and validity in the Chinese population (23,24).

We also collected information from BN patients regarding the duration of illness and frequency of binge eating-purging behavior.

MRI data acquisition

All MRI data were acquired on a 3.0 T MR scanner (Prisma, Siemens, Erlangen, Germany) equipped with a 64-channel phase-array head coil. Prior to the start of the scan, participants were told to close their eyes, remain calm and awake and keep their heads still. Earplugs and foam padding were used to minimize scanning noise and head movement, respectively. First, a routine brain axial T2 sequence was applied to screen for brain anatomic abnormalities. Anatomical T1-weighted images were then collected in the sagittal position using a three-dimensional magnetization-prepared rapid acquisition gradient-echo (MP-RAGE) sequence with the following parameters: repetition time (TR)/echo time (TE) =2,530 ms/2.98 ms; inversion time (TI) =1,100 ms; flip angle =7°; data matrix =256×256; voxel size =1×1×1 mm^3; field of view (FOV) =256×256 mm^2; slice thickness/gap =1.0 mm/1.0 mm; and slice number =192.

7080

Wang et al. Study on interhemispheric communication of BN

Functional images were recorded using an echo planar imaging (EPI) sequence with the following parameter settings: TR/TE, 2,000 ms/30 ms; flip angle, 90°; matrix, 64×64; FOV, 224×224 mm^2; slice thickness/gap, 3.5 mm/ 1 mm; slice number, 33; and time points, 240. And the DTI data were acquired with a diffusion sensitizing gradients applied along 64 non-linear directions (b=1,000 s/mm^2) together with an acquisition without diffusion weighting (b=0 s/mm^2). The parameters were 74 continuous slices parallel to the anterior commissure-posterior commissure line with a slice thickness of 2 mm and no gap; TR/TE, 8,500 ms/63 ms; matrix, 128×128; voxel size, 2×2×2 mm^3; FOV, 224×224 mm^2; and bandwidth, 2,232 Hz/Px.

During the scan, subjects were given additional voice reminders to prevent them from falling asleep. There were no reports of subjects dozing off or falling asleep during the scan.

Functional MRI data preprocessing

Preprocessing of resting-state fMRI (rs-fMRI) images was performed using Data Processing & Analysis for Brain Imaging (DPABI) software (http://rfmri.org/dpabi) based on Statistical Parametric Mapping (SPM12) (http://www.fil. ion.ucl.ac.uk/spm). The steps are briefly described below: (I) slice timing was performed on the remaining 230 volumes after the first ten volumes were discarded; (II) all subject head movements were corrected using a six-parameter rigid-body transformation, and any subjects with head movements that exceeded 2.0 mm in translation and 2.0° in rotation were eliminated. Given the potential confounding effect of head movements on the results, we also calculated the mean frame displacement (FD) for subsequent statistical analysis; (III) the T1-weighted images were then co-registered with the corresponding realigned functional images and segmented into: grey matter, WM and cerebrospinal fluid (CSF); (IV) the resulting images were normalized to standard Montreal Neurological Institute (MNI) space using the same parameters as for structural image normalization and subsequently resampled to a resolution of 3×3×3 mm^3; (V) the converted images were then band-pass filtered in 0.01–0.08 Hz; (VI) regression of interference signals generated by Friston 24 head motion parameters, CSF signals, and WM signals were conducted; (VII) detrending, and smoothing using a 6.0-mm full-width at half-maximum Gaussian kernel for each voxel. Data from two BN participants and one HC participants were eliminated from the head-movement correction step as their head movements met the aforementioned exclusion criteria. Finally, we included 42 patients with BN and 38 HC (80 participants in total) in the follow-up analyses.

VMHC calculation

The VMHC was also computed using the DPABI toolbox. To minimize geometric differences between the two hemispheres, the preprocessed images were registered to a bilateral hemispheric symmetric MNI template before being used in subsequent VMHC calculation. The interhemispheric homotopic connectivity was calculated as the Pearson correlation coefficient between the time series of a voxel and that of its mirror-symmetric voxel, which was known as the VMHC. The Fisher's r-to-z transformation was then applied to the correlation coefficients (25).

Seed-based FC calculation

Using the DPABI toolbox, the FC calculations were carried out in a seed-to-voxel manner. Brain regions with significant between-group differences in VMHC maps were used as seeds. By averaging the time series of all the voxels within each seed, the reference time series for each seed was derived. Next, the temporal correlation between the reference time series for each seed and the time series for each voxel throughout the entire brain was calculated to perform a voxel-wise FC analysis. Finally, Fisher's r-to-z transformation was applied to normalize the correlation coefficient maps to increase their normality.

CC structural calculation

DTI data of 80 subjects (42 BN patients and 38 HCs) included in the above steps were preprocessed. First, the raw DTI data was checked visually, no data with obvious artifacts were removed, and then the raw images were converted to NIfTI format. Whereafter, MP-PCA denoising was completed in DWI denoising of MRtrix3 using 5-voxel window (26). Then we applied MRtrix3's mrdegibbs for Gibbs deranging (27). After that, the inhomogeneity of B1 field was corrected by N4 algorithm using the DWI deviation corrected by MRtrix3 (28). The average intensity of all b=0 images was matched across each separate DWI sequence through the adjustment of the average intensity in the DWI series. Eddy distortion and subject's head movement were corrected in FSL software (version 6.0.3) (29). The spatial distortion of eddy current

was characterized by first-level linear model and second-level linear model. Next, we forcefully assigned the q space coordinates to the shell, separated the Field offset from the subject motion, and subsequently aligned the shells in the rear. We then ran Eddie's outlier replacement (30), replacing the data for the group that differs from the predicted value by more than 4 standard deviations with the predicted value. Finally, jac method was utilized for interpolation.

Subsequently, the fractional anisotropy (FA) value calculation and fiber tract quantification were conducted using the automated fiber quantification (AFQ) method proposed by Kruper *et al.* on AFQ software (https://github.com/yeatmanlab/pyAFQ) (31). This method provides comprehensive characterization of white matter fiber bundles. Compared with the conventional whole-tract analysis approach, this method can reveal the microstructural changes of white matter more sensitively. The primary processes were summarized as follows: (I) a deterministic streamline tracking algorithm was performed for whole brain tractography. The tracking was seeded at the thresholds with FA values >0.2 and turning angle <45°. (II) Fiber tract segmentation was performed in waypoint region of interest (ROI)-based procedure (32), and fiber tract refinement based on probability mapping was then conducted (33). (III) Fiber tracts cleaning into a compact tract spanning using the outlier rejection algorithm (34). (IV) Diffusion measurements were quantified by sampling each fiber bundle at 20 equidistant nodes. (V) Then, the major callosum forceps, the middle part of corpus callosum and minor callosum forceps, totally three whiter matter tracts were identified (32), and the mean value of average FA values for each node along with each tract were calculated. These values were then numerically weighted according to the consistency of the trajectory of the streamline in which they were located with other streamlines in the same fiber bundle, i.e., the contribution of the streamline in which they were located. (VI) Finally, we excluded subjects with missing data and adjusted the degrees of freedom for each fiber tract analysis as appropriate.

Statistical analyses

Group differences in demographic and behavioral and psychological data were compared using SPSS version 24.0. Kolmogorov-Smirnov test was applied for data normality test. The two-sample *t*-test was used to analyze data that fit the normal distribution; otherwise, the parametric test

(Mann-Whitney U test) was used. The Chi-squared test was used to test gender variables. The significance of group differences was established to $P<0.05$.

Using the SPM12 toolbox (https://www.fil.ion.ucl.ac.uk/spm/), a two-sample *t*-test with age, sex, education level, body mass index (BMI), and mean FD as covariates was performed to compared group differences in VMHC and FC across the whole brain. Cluster-level false discovery rate (FDR) correction was used for the multiple comparison corrections of the results, with a corrected threshold of $P<0.05$.

For AFQ analysis, we used two-sample t test to compare the group differences of mean FA values between HC and BN groups at 1–20 nodes along each fiber tracts. The multiple comparison corrections for results were performed using FDR correction with a corrected threshold of $P<0.05$.

Correlation analyses

We used the DPABI toolbox to extract VMHC and FC values for regions showing significant group differences. And we used the partial correlation analysis with age, sex, education level, BMI, and mean FD values as covariates to explore correlations between the imaging variables and clinical variables (including disease duration, binge eating-purging frequency and scores of DEBQ, EDI-BN, EAT-26, BDI and SAS). Then, we used the FDR correction to make multiple comparison correction for the results of correlation analysis, and the significant threshold was set at adjusted $P<0.05$.

We used the partial correlation analysis to investigate the correlations between altered VMHC values and mean FA values of altered fiber tracts (revealed by group comparisons). And we also performed the seed-based fiber tracking to make it clear that whether the white fiber between the bilateral brain regions with group difference in VMHC was through the area where the structure of the CC is changed. For the detailed steps for the seed-based fiber tracking, please refer to Appendix 1.

Moreover, to investigate whether the potential influence of VMHC on abnormal behaviors were mediated by abnormal WM microstructure of CC in the BN group or in all participants, we performed a standard three-variable mediation analysis on R package Mediation (version 4.5.0). The bias-correction significance of the mediation was estimated using the bootstrap strategy with 1,000 resampling iterations, and the statistically significance was set to $P<0.05$.

Table 1 Demographic and clinical characteristics of all participants

Variable	Bulimia nervosa patients (n=42)	Healthy controls (n=38)	P
Sex (F/M)	41/1	36/2	0.50[a]
Age (years)	23.76±5.45	24.97±2.34	0.21[b]
Education level (years)	16.40±1.75	17.24±2.22	0.07[b]
BMI (kg/m^2)	21.16±4.10	20.45±1.67	0.32[b]
Mean FD	0.12±0.06	0.12±0.04	0.45[b]
Illness duration (months)	41.38±43.29	NA	NA
Binge eating-purging frequency (times/week)	6.19±4.58	NA	NA
DEBQ-restrained	39.45±6.39	28.95±7.46	<0.001[b*]
DEBQ-emotional	47.33±10.95	26.24±9.63	<0.001[b*]
DEBQ-external	35.71±5.95	30.74±4.33	<0.001[b*]
EDI-BN	33.40±6.08	10.95±4.12	<0.001[b*]
EAT-26	46.10±11.80	12.11±10.14	<0.001[b*]
BDI	22.43±7.13	4.47±5.83	<0.001[b*]
SAS	54.78±11.62	33.64±8.63	<0.001[b*]

Data are presented as the mean ± SD. [a], Chi-square test; [b], two-sample t-test; *, the results were statistically significant (P<0.05). F, female; M, male; BMI, body mass index; FD, frame displacement; DEBQ, Dutch Eating Behavior Questionnaire; EDI-BN, bulimia subscale of the Eating Disorders Questionnaire; EAT, Eating Attitude Test; BDI, Beck Depression Inventory; SAS, Self-Assessment of Anxiety Scale; NA, not applicable.

Results

Demographic and clinical characteristics

Demographic and clinical data for BN patients and HCs are summarized in *Table 1*. A total of 42 BN patients and 38 HCs completed this study. There were no significant differences between the two groups in terms of age, sex, education level, BMI and FD. The BN group had higher scores on each scale and its subscales than the HC group.

Group differences in VMHC

Compared to HCs, patients with BN had significantly increased VMHC in the bilateral orbitofrontal cortex (OFC) (cluster size =70, peak t value =5.65, peak coordinates in MNI =±51, 42, –12) and middle temporal gyrus (MTG) (cluster size =52, peak t value =5.65, peak coordinates in MNI =±63, –63, 6). The results were corrected by the cluster-level FDR correction with a corrected threshold of P<0.05 and cluster size >42 (*Figure 1*).

Group differences in FC

Since the VMHC of both bilateral OFC and MTG showed significant differences between groups, we selected four seed points for seed-based FC analysis, namely, the left/right OFC and the left/right MTG, respectively. Compared with the HC group, the BN group displayed increased FC between the left OFC and right OFC, bilateral MTG, left middle occipital gyrus (MOG) and right precuneus (PCUN); between the right OFC and left cerebellum crus II and right PCUN; and between the left MTG and the right inferior temporal gyrus (ITG), right cerebellum lobule VI and right medial superior frontal gyrus (SFGmed) (cluster-level FDR correction with a corrected threshold of P<0.05 and cluster size >164, >167 and >117, respectively) (*Table 2* and *Figure 2*).

Group differences in WM microstructure of CC

Compared to HCs, patients with BN showed a significant decrease in WM FA values of the middle part of CC
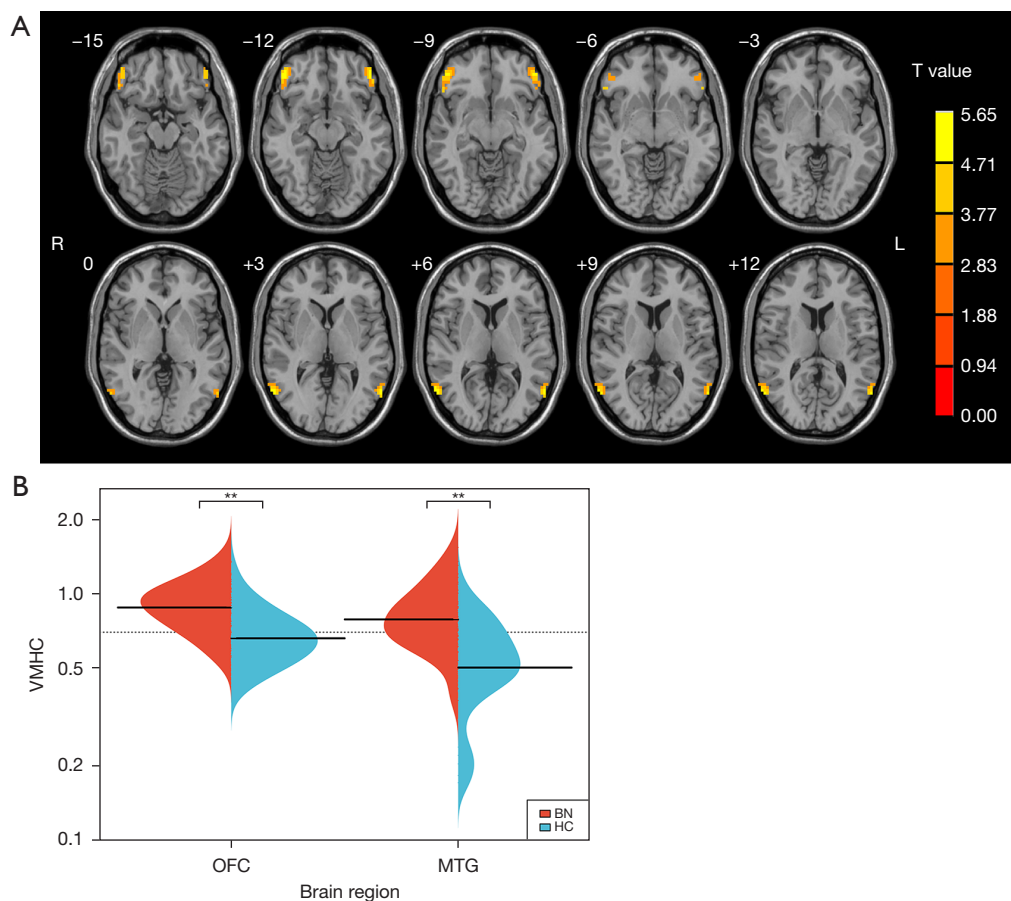
Figure 1 Group differences of VMHC between BN patients and HCs. (A) The warm-color areas represent brain regions where VMHC values of BN patients were significantly higher than those of HCs. (B) VMHC z scores of BN *vs.* HC in regions with group differences of VMHC. (cluster-level FDR correction with a corrected threshold of P<0.05). VMHC, voxel-mirrored homotopic connectivity; BN, bulimia nervosa; HC, healthy control; OFC, orbitofrontal cortex; MTG, middle temporal gyrus; FDR, false discovery rate. **, The results were statistically significant (P<0.01).

(CCMid) (node 18) (FDR correction with a corrected threshold of P<0.05) (*Figure 3*).

Correlations between VMHC alterations and CC alterations

In BN patients, the VMHC values of OFC and MTG showed no correlations with the FA values of the CCMid. And the seed-based fiber tracking showed that the white fibers between the bilateral OFC and MTG were not through the area where the structure of the CC was changed (i.e., CCMid). In the mediation analysis, we did not find a mediating role for the WM microstructure of CC in the effect of VMHC on abnormal behaviors.

Correlations between imaging variables and clinical variables

In BN group, there was no correlation between the FA values of CCMid or VMHC values of OFC/MTG and clinical data in this study. The correlations between altered FC and clinical data did not survive the FDR correction (adjusted P<0.05). Thus, the following results show a trend of correlation at P<0.05 (uncorrected). The FC values of left OFC and left MOG showed a positive correlation trend with binge eating-purging frequency (r=0.405, P=0.009, uncorrected). The FC values of left OFC and right PCUN were positively correlated with both binge eating-purging frequency (r=0.339, P=0.03, uncorrected) and DEBQ-

Table 2 Group differences in seed-based FC (BN *vs.* HC)

Seed region	Regions with altered FC	Cluster size	Peak t value	Peak coordinates (MNI)		
				X	Y	Z
OFC.L	OFC.R	210	4.57	51	36	−12
	MTG.L	180	4.92	−54	−15	−15
	MTG.R	165	4.59	42	−15	−15
	MOG.L	282	4.92	−6	−102	6
	PCUN.R	219	4.43	9	−57	33
OFC.R	Cerebellum Crus2.L	226	4.44	−18	−81	−36
	PCUN.R	167	4.61	0	−81	48
MTG.L	ITG.R	137	5.19	54	−42	−27
	Cerebellum 6.R	117	4.32	21	−75	−18
	SFGmed.R	169	4.46	6	69	−9

FC, functional connectivity; BN, bulimia nervosa; HC, healthy control; MNI, Montreal Neurological Institute; OFC.L, left orbitofrontal cortex; OFC.R, right orbitofrontal cortex; MTG.L, left middle temporal gyrus; MTG.R, right middle temporal gyrus; MOG.L, left middle occipital gyrus; PCUN.R, right precuneus; Cerebellum Crus2.L, left cerebellum crus II; ITG.R, right inferior temporal gyrus; Cerebellum 6.R, right cerebellum lobule VI; SFGmed.R, right medial superior frontal gyrus.

emotional scores at a trend level (r=0.345, P=0.027, uncorrected). In addition, the FC values of left MTG and right ITG were positively correlated with DEBQ-emotional scores at a trend level (r=0.384, P=0.013, uncorrected) (*Figure 4*).

Discussion

In this study, we explored BN-related interhemispheric communications from both functional and structural perspectives. Consistent with our hypothesis, we found specific alterations of interhemispheric communication in BN as well as abnormal FC between regions with aberrant VMHC and other specific areas of the brain. There were three primary findings: (I) BN patients exhibited enhanced VMHC of the bilateral OFC and MTG, while decreased FA of the CC compared to HCs. (II) And the OFC and MTG showed hyperconnectivity with visual, reward-related and self-referential regions. (III) Hyperconnectivity between OFC and other regions exhibited significant correlation with binge eating-purging and emotional-eating behaviors in BN patients.

The aberrant WM properties of CC observed in the present study are in accordance with previous studies on BN (35), and in those studies, researchers also found a correlation between FA reduction in CC and the severity of symptoms (36). Hence, we can reasonably postulate that impaired CC WM microstructure is associated with the neural mechanism underlying BN. Structural deficits in the CC may lead to variations in VMHC, which was supported by the aberrant functional coherence between hemispheres in callosotomized patients (37). Given the importance of the CC in modulating functional coordination between hemispheres, this study had also explored the correlation between FA value of CC and VMHC, but did not find them to be correlated. And we found that the white fibers between the bilateral OFC and MTG were not through the area where the structure of the CC was changed. We cautiously speculate that the independence between the structural alterations in CC and the alterations in VMHC may be related to the indexes we used or the dimensions we explored in the present study, and the association between the CC structure and interhemispheric functional connectivity of BN needs to be further explored in future studies with different analysis techniques and analysis dimensions and with larger sample sizes.

This study found enhanced VMHC in the OFC of patients with BN. Parallelly, we previously reported increased OFC volume in BN patients (38). Mounting researches have proved the involvement of the OFC in the neural mechanism of BN from the perspectives in brain activation pattern (39), structural network properties (11)
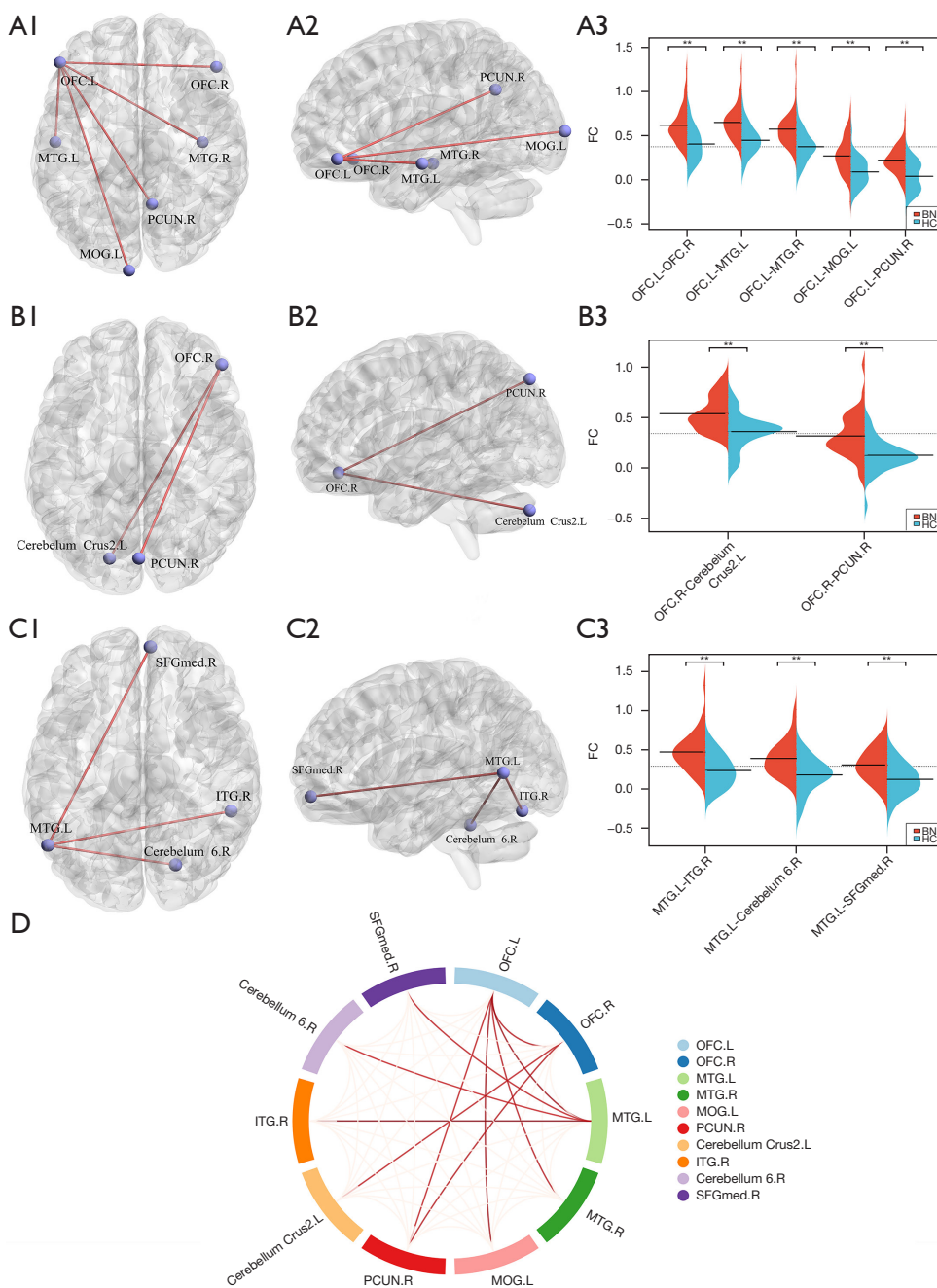
Figure 2 Group differences of seed-based FC between BN patients and HCs (seeds regions are OFC.L, OFC.R and MTG.L, respectively). (A1-A2) Axial and sagittal views of the results of seed-based FC analysis with the OFC.L set as the seed. (A3) FC z values of BN *vs.* HC between OFC.L and OFC.R/MTG.L/MTG.R/MOG.R/PCUN.R. (B1-B2) Axial and sagittal views of the results of seed-based FC analysis when with the OFC.R set as the seed. (B3) FC z values of BN *vs.* HC between OFC.R and Cerebellum Crus 2.L/PCUN.R. (C1-C2) Axial and sagittal views of seed-based FC results with the MTG.L set as the seed. (C3) FC z values of BN *vs.* HC between MTG.L and ITG.R/Cerebellum 6.R/ SFGmed.R. (D) Seed-based FC patterns, as evidenced in this "connectome ring" (cluster-level FDR correction with a corrected threshold of P<0.05). FC, functional connectivity; BN, bulimia nervosa; HC, healthy control; OFC.L, left orbitofrontal cortex; OFC.R, right orbitofrontal cortex; MTG.L, left middle temporal gyrus; MTG.R, right middle temporal gyrus; MOG.L left middle occipital gyrus; PCUN.R, right precuneus; Cerebellum Crus2.L, left cerebellum crus II; ITG.R, right inferior temporal gyrus; Cerebellum 6.R, right cerebellum lobule VI; SFGmed.R, right medial superior frontal gyrus; FDR, false discovery rate. **, The results were statistically significant (P<0.01).

7086

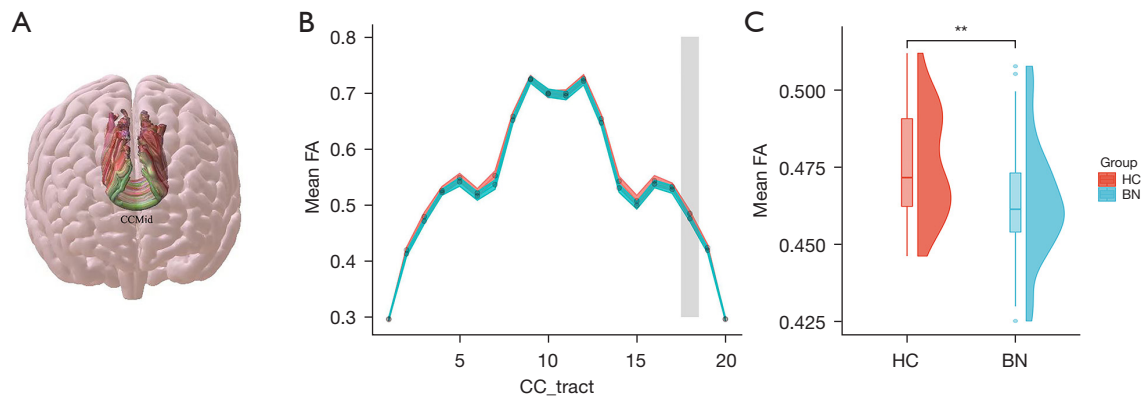Wang et al. Study on interhemispheric communication of BN

Figure 3 Group differences of FA values in CC between BN patients and HCs. (A) Anatomical diagram of the CCMid. (B) Node diagram of the CCMid fiber tract (shaded areas indicate the regions with altered microstructure). (C) Mean FA values of BN *vs.* HC in CCMid. (FDR correction with a corrected threshold of P<0.05). FA, fractional anisotropy; BN, bulimia nervosa; HC, healthy control; CC, corpus callosum; CCMid, middle part of corpus callosum; FDR, false discovery rate. **, The results were statistically significant (P<0.01).
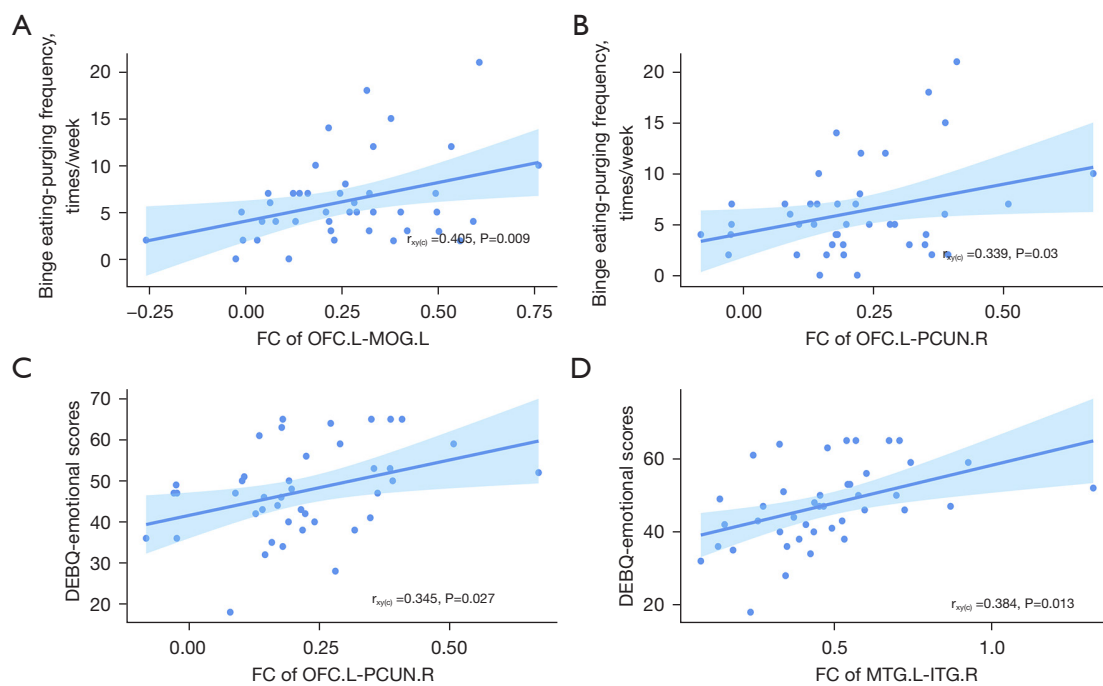
Figure 4 Correlations between imaging variables and behavioral manifestations in BN patients. (A) Correlation of FC (OFC.L-MOG.L) with binge eating-purging times per week. (B) Correlation of FC (OFC.L-PCUN.R) with binge eating-purging times per week. (C) Correlation of FC (OFC.L-PCUN.R) with DEBQ-emotional scores. (D) Correlation of FC (MTG.L-ITG.R) with DEBQ-emotional scores. These results were not corrected for multiple comparisons. BN, bulimia nervosa; OFC.L, left orbitofrontal cortex; MOG.L, left middle occipital gyrus; PCUN.R, right precuneus; DEBQ, Dutch Eating Behavior Questionnaire; MTG.L, left middle temporal gyrus; ITG.R, right inferior temporal gyrus.

and FC (8). OFC is involved in hedonic food processing and plays a central role in food value-directed eating behavior (40). It represents the affective value of reinforcers in the board context of decision making (41). Although the pathophysiological mechanisms of BN remain unclear, abnormal brain reward mechanism has been widely reported. In patients with binge eating disorder, OFC activation was reported to be positively correlated with reward sensitivity when viewing food images (42). Moreover, research has suggested a possible link between eating disorder subjects' preternatural eating behavior and their supposedly disorganized reward processes (43). The enhanced VMHC of OFC may be interpreted as an indexing tendency towards increased coordinated processing in reward. Since increased reward sensitivity (44) and reward dependence (45) are prominent and characteristic clinical manifestations of BN, we speculate that such manifestations require excessive functional coordination of brain regions related to reward, and VMHC enhancement of OFC may be the neural basis of such clinical manifestations. OFC may be a potential therapeutic target to reverse the corresponding behavioral abnormalities.

Another area identified to have increased VMHC in this study is the MTG, specifically the part located in the occipitotemporal junction. This area belongs to the extrastriate body area (EBA), which is a body-selective visual cortex that responds strongly to images of body parts and is dedicated to the visual perception and processing of body information (46). Vocks et al. (47) found increased EBA activation in patients with AN following cognitive-behavioral body image treatment, supporting its pivotal role in body image perception. Of note, excessive preoccupation with body shape and distorted body image perception is another robust characteristic of BN in addition to abnormal eating behavior (48). A meta-analysis based on 42 articles concluded that both AN and BN patients misjudged their body size (49). EBA alterations are highly associated with body size distortion; Mohr et al. (50) observed that the EBA activity of healthy subjects increased when they viewed body size distortion, while such modulation was absent in the BN group. Therefore, the enhancement of VMHC may imply an excessive interhemispheric exchange of information about the perception of body shape, which leads to an overconcern for body shape. And MTG is a potential target for reversing the morbid body image perception in patients with BN.

It has recently been suggested that higher levels of interhemispheric functional homotopy in a given region

signify its crucial role in the regional hierarchy within brain network and that strong functional homotopy may be responsible for enabling more reliable integration of information (17). Therefore, we presume that the OFC and MTG might be the key nodes in the reorganized neural network of BN. Subsequent seed-based FC analysis confirmed our hypothesis, revealing abnormal FC between regions with abnormal VMHC and other specific regions, more specifically, between the OFC and MTG, MOG, PCUN, cerebellum and between MTG and ITG, SFGmed and cerebellum. Both the MTG and MOG belong to the occipitotemporal network, which is associated with body image perception (51). The occipital cortex, an area that regulates the visual perception of body shape, is thought to be associated with the perception of inappropriate body image (52). The ITG, a key component in visual comprehension, is connected posteriorly to the inferior occipital gyrus, perceiving and processing visual stimuli amplified in the occipital region (53). Receiving and processing body image input relies heavily on the primary sensorimotor cortex as well as temporo-parietal-occipital visual-related cortex (54,55). In BN, the integrity of the WM of uncinate fasciculi, which connects the visual-related areas of the prefrontal, temporal and occipital cortices, was compromised, and reduced FA in this tract was most pronounced in individuals most concerned about their body shape (36). The SFGmed is a part of the ventral medial to the prefrontal cortex (vmPFC) (56). A task-state fMRI study by Fischer et al. (57) detected reduced activity in reward-related areas in response to food cues in patients with BN, including the vmPFC, anterior cingulate cortex and amygdala. The vmPFC exerts a wide range of regulatory effects on food valuation processes, thereby influencing dietary decision-making and control (58). Our study links the FC alterations among regions associated with processing of reward (OFC and vmPFC) and body image information (MTG, MOG and ITG). Given that patients with eating disorders consider their body shape as a predominant referent for inferring personal value (59), we speculate that excessive attention to body image in BN patients may induce the recoding of the reward value of food, which may be relevant to the pathogenesis and maintenance of binge-eating behavior. This speculation is further supported by the correlation trend between the FC (the OFC-MOG) and the frequency of binge eating-purging (reflects the severity of disease).

The PCUN plays a central role in a range of higher cognitive activities and is a core component of the

DMN (60). DMN is responsible for self-referential thinking, and its increased activity correlates with over-focusing on negative aspects of oneself (61). Behavioral studies revealed that, for BN patients, the purpose of consuming large amounts of food is to relieve their negative emotion, which was partly aroused by excessive focus on negative self-referential thoughts (62,63). Taken together, such hyperconnectivity reflects the potential synergistic effect of self-negative cognition and abnormal reward mechanisms on eating behavior, and the correlation trend of such hyperconnectivity with the binge eating-purging frequency and emotional eating behavior shown in this study further supports this presumption.

Intriguingly, we also found increased FC between the OFC/MTG and the cerebellum. Although little is known about the involvement of the cerebellum in the neural mechanisms of BN, recent studies of the cerebellum in the context of eating and feeding behavior have demonstrated that the cerebellum is implicated in food-related processing (64,65). The cerebellum in AN patients displayed hyperactivation when processing food stimuli (66). Even though our study found abnormal FC between the cerebrum and cerebellum, the exact mechanism of cerebello-cerebral connectivity in BN is not fully expounded and further research is needed to clarify such connectivity pattern.

The present study has some limitations that should be acknowledged. Firstly, though our study found that FC between OFC and other specific regions was associated with abnormal eating behavior in BN patients at a trend level, the precise neural mechanisms need to be elucidated with a more targeted experimental design. Second, our analysis was based on cross-sectional data. In the future, we plan to use a longitudinal design to analyze dynamic changes in interhemispheric coordination over time in BN. Finally, the sample size of this study was modest, which limited its statistical power. Studies with more participants are needed to further validate the reliability of our findings.

Conclusions

In conclusion, this study revealed aberrant interhemispheric communications from both structural and functional perspectives in BN. We found that the WM microstructure of CC, the major WM fiber tract connecting the two hemispheres, was impaired, and that the OFC and MTG had enhanced VMHC. The changes in interhemispheric functional and structural connectivity of BN may be independent of each other. As the key nodes in the reorganized network, the OFC and MTG showed abnormal functional hyperconnectivity with regions related to reward processing, body shape perception, and self-reference. These findings may provide novel insight into the neural circuitry underlying the complex behavioral deficits in BN and provide potential targets for treatment.

Footnote

Conflicts of Interest: All authors have completed the ICMJE uniform disclosure form (available at https://qims. amegroups.com/article/view/10.21037/qims-23-18/coif). The authors have no conflicts of interest to declare.

Ethical Statement: The authors are accountable for all aspects of the work in ensuring that questions related to the accuracy or integrity of any part of the work are appropriately investigated and resolved. The trial was conducted in accordance with the Declaration of Helsinki (as revised in 2013). The study was approved by the Ethics Committee of the Beijing Friendship Hospital (No. 2021-P2-052-01), and all participants signed written informed consent.

References

1. Castillo M, Weiselberg E. Bulimia Nervosa/Purging Disorder. Curr Probl Pediatr Adolesc Health Care 2017;47:85-94.

2. Treasure J, Claudino AM, Zucker N. Eating disorders. Lancet 2010;375:583-93.

3. Steinhausen HC, Weber S. The outcome of bulimia nervosa: findings from one-quarter century of research. Am J Psychiatry 2009;166:1331-41.

4. Smink FR, van Hoeken D, Hoek HW. Epidemiology of eating disorders: incidence, prevalence and mortality rates. Curr Psychiatry Rep 2012;14:406-14.

5. Lee JE, Namkoong K, Jung YC. Impaired prefrontal cognitive control over interference by food images in binge-eating disorder and bulimia nervosa. Neurosci Lett 2017;651:95-101.

6. Berner LA, Marsh R. Frontostriatal circuits and the development of bulimia nervosa. Front Behav Neurosci 2014;8:395.

7. Uher R, Murphy T, Friederich HC, Dalgleish T, Brammer MJ, Giampietro V, Phillips ML, Andrew CM, Ng VW, Williams SC, Campbell IC, Treasure J. Functional neuroanatomy of body shape perception in healthy and eating-disordered women. Biol Psychiatry 2005;58:990-7.

8. Wang JN, Tang LR, Li WH, Zhang XY, Shao X, Wu PP, Yang ZM, Wu GW, Chen Q, Wang Z, Zhang P, Li ZJ, Wang Z. Regional Neural Activity Abnormalities and Whole-Brain Functional Connectivity Reorganization in Bulimia Nervosa: Evidence From Resting-State fMRI. Front Neurosci 2022;16:858717.

9. Wang L, Bi K, Song Z, Zhang Z, Li K, Kong QM, Li XN, Lu Q, Si TM. Disturbed Resting-State Whole-Brain Functional Connectivity of Striatal Subregions in Bulimia Nervosa. Int J Neuropsychopharmacol 2020;23:356-65.

10. Domakonda MJ, He X, Lee S, Cyr M, Marsh R. Increased Functional Connectivity Between Ventral Attention and Default Mode Networks in Adolescents With Bulimia Nervosa. J Am Acad Child Adolesc Psychiatry 2019;58:232-41.

11. Wang L, Bi K, An J, Li M, Li K, Kong QM, Li XN, Lu Q, Si TM. Abnormal structural brain network and hemisphere-specific changes in bulimia nervosa. Transl Psychiatry 2019;9:206.

12. Zhang Y, Huang Y, Liu N, Wang Z, Wu J, Li W, Xia J, Liu Z, Li Y, Hao Y, Huo J. Abnormal interhemispheric functional connectivity in patients with primary dysmenorrhea: a resting-state functional MRI study. Quant Imaging Med Surg 2022;12:1958-67.

13. Zhao W, Zhu D, Zhang Y, Zhang C, Zhang B, Yang Y, Zhu J, Yu Y. Relationship between illness duration, corpus callosum changes, and sustained attention dysfunction in major depressive disorder. Quant Imaging Med Surg 2021;11:2980-93.

14. Qiu YW, Jiang GH, Ma XF, Su HH, Lv XF, Zhuo FZ. Aberrant interhemispheric functional and structural connectivity in heroin-dependent individuals. Addict Biol 2017;22:1057-67.

15. Roland JL, Snyder AZ, Hacker CD, Mitra A, Shimony JS, Limbrick DD, Raichle ME, Smyth MD, Leuthardt EC. On the role of the corpus callosum in interhemispheric functional connectivity in humans. Proc Natl Acad Sci U S A 2017;114:13278-83.

16. Zuo XN, Kelly C, Di Martino A, Mennes M, Margulies DS, Bangaru S, Grzadzinski R, Evans AC, Zang YF, Castellanos FX, Milham MP. Growing together and growing apart: regional and sex differences in the lifespan developmental trajectories of functional homotopy. J Neurosci 2010;30:15034-43.

17. Shen K, Mišić B, Cipollini BN, Bezgin G, Buschkuehl M, Hutchison RM, Jaeggi SM, Kross E, Peltier SJ, Everling S, Jonides J, McIntosh AR, Berman MG. Stable long-range interhemispheric coordination is supported by direct anatomical projections. Proc Natl Acad Sci U S A 2015;112:6473-8.

18. Davis SW, Cabeza R. Cross-hemispheric collaboration and segregation associated with task difficulty as revealed by structural and functional connectivity. J Neurosci 2015;35:8191-200.

19. Sheehan DV, Lecrubier Y, Sheehan KH, Amorim P, Janavs J, Weiller E, Hergueta T, Baker R, Dunbar GC. The Mini-International Neuropsychiatric Interview (M.I.N.I.): the development and validation of a structured diagnostic psychiatric interview for DSM-IV and ICD-10. J Clin Psychiatry 1998;59 Suppl 20:22-33;quiz 34-57.

20. Wu S, Cai T, Luo X. Validation of the Dutch Eating Behavior Questionnaire (DEBQ) in a sample of Chinese adolescents. Psychol Health Med 2017;22:282-8.

21. Lee S, Lee AM, Leung T, Yu H. Psychometric properties of the Eating Disorders Inventory (EDI-1) in a nonclinical Chinese population in Hong Kong. Int J Eat Disord 1997;21:187-94.

22. Kang Q, Chan RCK, Li X, Arcelus J, Yue L, Huang J, Gu L, Fan Q, Zhang H, Xiao Z, Chen J. Psychometric Properties of the Chinese Version of the Eating Attitudes Test in Young Female Patients with Eating Disorders in

7090

Wang et al. Study on interhemispheric communication of BN

Mainland China. Eur Eat Disord Rev 2017;25:613-7.

23. Shek DT. Reliability and factorial structure of the Chinese version of the Beck Depression Inventory. J Clin Psychol 1990;46:35-43.

24. Zung WW. A rating instrument for anxiety disorders. Psychosomatics 1971;12:371-9.

25. Kelly C, Zuo XN, Gotimer K, Cox CL, Lynch L, Brock D, Imperati D, Garavan H, Rotrosen J, Castellanos FX, Milham MP. Reduced interhemispheric resting state functional connectivity in cocaine addiction. Biol Psychiatry 2011;69:684-92.

26. Veraart J, Novikov DS, Christiaens D, Ades-Aron B, Sijbers J, Fieremans E. Denoising of diffusion MRI using random matrix theory. Neuroimage 2016;142:394-406.

27. Kellner E, Dhital B, Kiselev VG, Reisert M. Gibbs-ringing artifact removal based on local subvoxel-shifts. Magn Reson Med 2016;76:1574-81.

28. Tustison NJ, Avants BB, Cook PA, Zheng Y, Egan A, Yushkevich PA, Gee JC. N4ITK: improved N3 bias correction. IEEE Trans Med Imaging 2010;29:1310-20.

29. Andersson JLR, Sotiropoulos SN. An integrated approach to correction for off-resonance effects and subject movement in diffusion MR imaging. Neuroimage 2016;125:1063-78.

30. Andersson JLR, Graham MS, Zsoldos E, Sotiropoulos SN. Incorporating outlier detection and replacement into a non-parametric framework for movement and distortion correction of diffusion MR images. Neuroimage 2016;141:556-72.

31. Kruper J, Yeatman JD, Richie-Halford A, Bloom D, Grotheer M, Caffarra S, Kiar G, Karipidis II, Roy E, Chandio BQ, Garyfallidis E, Rokem A. Evaluating the Reliability of Human Brain White Matter Tractometry. Apert Neuro 2021;1.

32. Wakana S, Caprihan A, Panzenboeck MM, Fallon JH, Perry M, Gollub RL, Hua K, Zhang J, Jiang H, Dubey P, Blitz A, van Zijl P, Mori S. Reproducibility of quantitative tractography methods applied to cerebral white matter. Neuroimage 2007;36:630-44.

33. Yeh FC, Panesar S, Fernandes D, Meola A, Yoshino M, Fernandez-Miranda JC, Vettel JM, Verstynen T. Population-averaged atlas of the macroscale human structural connectome and its network topology. Neuroimage 2018;178:57-68.

34. Chang LC, Jones DK, Pierpaoli C. RESTORE: robust estimation of tensors by outlier rejection. Magn Reson Med 2005;53:1088-95.

35. Mettler LN, Shott ME, Pryor T, Yang TT, Frank GK. White matter integrity is reduced in bulimia nervosa. Int J Eat Disord 2013;46:264-73.

36. He X, Stefan M, Terranova K, Steinglass J, Marsh R. Altered White Matter Microstructure in Adolescents and Adults with Bulimia Nervosa. Neuropsychopharmacology 2016;41:1841-8.

37. Johnston JM, Vaishnavi SN, Smyth MD, Zhang D, He BJ, Zempel JM, Shimony JS, Snyder AZ, Raichle ME. Loss of resting interhemispheric functional connectivity after complete section of the corpus callosum. J Neurosci 2008;28:6453-8.

38. Li WH, Tang LR, Wang M, Wang JN, Guo T, He Q, He YY, Lv ZL, Chen Q, Wang Z, Li XH, Zhang P, Li ZJ, Wang ZC. Altered gray matter volume and functional connectivity in medial orbitofrontal cortex of bulimia nervosa patients: A combined VBM and FC study. Front Psychiatry 2022;13:963092.

39. Marsh R, Steinglass JE, Gerber AJ, Graziano O'Leary K, Wang Z, Murphy D, Walsh BT, Peterson BS. Deficient activity in the neural systems that mediate self-regulatory control in bulimia nervosa. Arch Gen Psychiatry 2009;66:51-63.

40. Schoenbaum G, Takahashi Y, Liu TL, McDannald MA. Does the orbitofrontal cortex signal value? Ann N Y Acad Sci 2011;1239:87-99.

41. Suzuki S, Cross L, O'Doherty JP. Elucidating the underlying components of food valuation in the human orbitofrontal cortex. Nat Neurosci 2017;20:1780-6.

42. Schienle A, Schäfer A, Hermann A, Vaitl D. Binge-eating disorder: reward sensitivity and brain activation to images of food. Biol Psychiatry 2009;65:654-61.

43. Morales I, Berridge KC. 'Liking' and 'wanting' in eating and food reward: Brain mechanisms and clinical implications. Physiol Behav 2020;227:113152.

44. Simon JJ, Skunde M, Walther S, Bendszus M, Herzog W, Friederich HC. Neural signature of food reward processing in bulimic-type eating disorders. Soc Cogn Affect Neurosci 2016;11:1393-401.

45. Monteleone AM, Castellini G, Volpe U, Ricca V, Lelli L, Monteleone P, Maj M. Neuroendocrinology and brain imaging of reward in eating disorders: A possible key to the treatment of anorexia nervosa and bulimia nervosa. Prog Neuropsychopharmacol Biol Psychiatry 2018;80:132-42.

46. Downing PE, Jiang Y, Shuman M, Kanwisher N. A cortical area selective for visual processing of the human body. Science 2001;293:2470-3.

47. Vocks S, Schulte D, Busch M, Grönemeyer D, Herpertz S,

Suchan B. Changes in neuronal correlates of body image processing by means of cognitive-behavioural body image therapy for eating disorders: a randomized controlled fMRI study. Psychol Med 2011;41:1651-63.

48. Kaye W. Neurobiology of anorexia and bulimia nervosa. Physiol Behav 2008;94:121-35.

49. Mölbert SC, Klein L, Thaler A, Mohler BJ, Brozzo C, Martus P, Karnath HO, Zipfel S, Giel KE. Depictive and metric body size estimation in anorexia nervosa and bulimia nervosa: A systematic review and meta-analysis. Clin Psychol Rev 2017;57:21-31.

50. Mohr HM, Röder C, Zimmermann J, Hummel D, Negele A, Grabhorn R. Body image distortions in bulimia nervosa: investigating body size overestimation and body size satisfaction by fMRI. Neuroimage 2011;56:1822-31.

51. Fontan A, Cignetti F, Nazarian B, Anton JL, Vaugoyeau M, Assaiante C. How does the body representation system develop in the human brain? Dev Cogn Neurosci 2017;24:118-28.

52. Favaro A, Santonastaso P, Manara R, Bosello R, Bommarito G, Tenconi E, Di Salle F. Disruption of visuospatial and somatosensory functional connectivity in anorexia nervosa. Biol Psychiatry 2012;72:864-70.

53. Lin Q, Zhu FY, Shu YQ, Zhu PW, Ye L, Shi WQ, Min YL, Li B, Yuan Q, Shao Y. Altered brain network centrality in middle-aged patients with retinitis pigmentosa: A resting-state functional magnetic resonance imaging study. Brain Behav 2021;11:e01983.

54. Bracci S, Caramazza A, Peelen MV. Representational Similarity of Body Parts in Human Occipitotemporal Cortex. J Neurosci 2015;35:12977-85.

55. Mesulam MM. From sensation to cognition. Brain 1998;121 (Pt 6):1013-52.

56. Konova AB, Parvaz MA, Bernstein V, Zilverstand A, Moeller SJ, Delgado MR, Alia-Klein N, Goldstein RZ. Neural mechanisms of extinguishing drug and pleasant cue associations in human addiction: role of the VMPFC. Addict Biol 2019;24:88-99.

57. Fischer S, Breithaupt L, Wonderlich J, Westwater ML, Crosby RD, Engel SG, Thompson J, Lavender J, Wonderlich S. Impact of the neural correlates of stress and cue reactivity on stress related binge eating in the natural environment. J Psychiatr Res 2017;92:15-23.

58. Schmidt L, Tusche A, Manoharan N, Hutcherson C, Hare T, Plassmann H. Neuroanatomy of the vmPFC and dlPFC Predicts Individual Differences in Cognitive Regulation During Dietary Self-Control Across Regulation Strategies. J Neurosci 2018;38:5799-806.

59. Siep N, Jansen A, Havermans R, Roefs A. Cognitions and emotions in eating disorders. Curr Top Behav Neurosci 2011;6:17-33.

60. Li R, Utevsky AV, Huettel SA, Braams BR, Peters S, Crone EA, van Duijvenvoorde ACK. Developmental Maturation of the Precuneus as a Functional Core of the Default Mode Network. J Cogn Neurosci 2019;31:1506-19.

61. Hamilton JP, Furman DJ, Chang C, Thomason ME, Dennis E, Gotlib IH. Default-mode and task-positive network activity in major depressive disorder: implications for adaptive and maladaptive rumination. Biol Psychiatry 2011;70:327-33.

62. Puttevils L, Vanderhasselt MA, Horczak P, Vervaet M. Differences in the use of emotion regulation strategies between anorexia and bulimia nervosa: A systematic review and meta-analysis. Compr Psychiatry 2021;109:152262.

63. Fischer S, Wonderlich J, Breithaupt L, Byrne C, Engel S. Negative urgency and expectancies increase vulnerability to binge eating in bulimia nervosa. Eat Disord 2018;26:39-51.

64. Zhu JN, Wang JJ. The cerebellum in feeding control: possible function and mechanism. Cell Mol Neurobiol 2008;28:469-78.

65. Amianto F, Caroppo P, D'Agata F, Spalatro A, Lavagnino L, Caglio M, Righi D, Bergui M, Abbate-Daga G, Rigardetto R, Mortara P, Fassino S. Brain volumetric abnormalities in patients with anorexia and bulimia nervosa: a voxel-based morphometry study. Psychiatry Res 2013;213:210-6.

66. Horndasch S, Roesch J, Forster C, Dörfler A, Lindsiepe S, Heinrich H, Graap H, Moll GH, Kratz O. Neural processing of food and emotional stimuli in adolescent and adult anorexia nervosa patients. PLoS One 2018;13:e0191059.

Appendix 1 Seed-based fiber tracking

To generate seed regions for tractography, whole-brain tractography was performed using the iFOD2 algorithm, which employs second-order Integration over fiber orientation distributions. A total of ten million streamlines were randomly seeded throughout the entire brain volume. Regions of interest (ROIs) were defined on the fractional anisotropy (FA) image, i.e., the brain regions with group difference in voxel-mirrored homotopic connectivity (VMHC). The orbital part of the inferior frontal cortex (OFC) and middle temporal gyrus (MTG) regions exhibiting significant group differences (VMHC) were registered into each subject's T1 space and used as inclusion regions in separate runs (two runs in total, one for OFC and one for MTG). Tracking was terminated upon the initiation of a cumulative count of 100,000 tracks.

The MRtrix software package was employed for the implementation of tractography. The probabilistic "bootstrap" algorithms were utilized for diffusion tensor imaging (DTI)-based tractography, while probabilistic constrained spherical deconvolution (CSD)-derived tractography was performed using the iFOD2 algorithm. The default settings in MRtrix were employed for these tractography methods. Tract density maps were generated in the native structural brain space using the MRtrix software package, and a threshold of 10 streamlines per voxel was applied to mitigate the inclusion of potentially spurious tracts.

In summary, bilateral MTG and OFC regions were used as seed regions, respectively, for targeted fiber tracking. And then observe whether the tracked target fiber bundles traverse the corpus callosum structurally altered region (CCMid).